Letter

# Determining bifurcations to explosive synchronization for networks of coupled oscillators with higher-order interactions

Lauren D. Smith* and Penghao Liu
*Department of Mathematics, University of Auckland, Auckland 1142, New Zealand*

(Received 24 October 2023; accepted 22 January 2024; published 23 February 2024)

We determine bifurcations from gradual to explosive synchronization in coupled oscillator networks with higher-order coupling using self-consistency analysis. We obtain analytic bifurcation values for generic symmetric natural frequency distributions. We show that nonsynchronized, drifting, oscillators are non-negligible and play a crucial role in bifurcation. As such, the entire natural frequency distribution must be accounted for, rather than just the shape at the center. We verify our results for Lorentzian- and Gaussian-distributed natural frequencies.

DOI: 10.1103/PhysRevE.109.L022202

Many natural phenomena and engineering applications can be described as networks of coupled oscillators, for example, the firing of neurons in the brain [1,2] and the dynamics of power grids [3–6]. Classically, only pairwise interactions were considered, but it has recently been brought to light that many real-world networks have higher-order interactions [7–9] such that nodes interact as triplets or quadruplets, or larger groups. Moreover, it has been shown that these higher-order interactions yield fundamentally different dynamics than can be achieved with only pairwise coupling [10,11]. In particular, for coupled oscillators, higher-order interactions have been shown to generate abrupt, explosive, transitions to synchronization that do not generically occur with pairwise coupling [9–17]. These explosive transitions have been studied in detail for many classes of higher-order interactions, with most studies considering only Lorentzian-distributed natural frequencies due to their amenability to the Ott-Antonsen ansatz [18,19].

Here we determine critical parameter sets for general natural frequency distributions at which the onset of synchronization bifurcates from a gradual smooth transition to an abrupt explosive transition. We do this using a self-consistency approach akin to that of Kuramoto's [20,21]. In Kuramoto's famous result, the onset of synchronization for symmetric frequency distributions is governed entirely by the shape of the frequency distribution at its center. We show that this is not the case for general higher-order dynamics because the population of "drifters" (oscillators that do not synchronize) cannot be neglected. As such, the entirety of the frequency distribution must be accounted for. We verify that our methodology recovers known formulas for Lorentzian-distributed frequencies and uncover analytic bifurcation values for Gaussian-distributed frequencies.

We begin by considering an all-to-all coupled network, with higher-order dynamics given by

$$\dot{\theta}_i = \omega_i + \frac{K_1}{N}\sum_{j=1}^{N}\sin(\theta_j-\theta_i) + \frac{K_2}{N^2}\sum_{j,l=1}^{N}\sin(2\theta_j-\theta_l-\theta_i) + \frac{K_3}{N^3}\sum_{j,l,m=1}^{N}\sin(\theta_j+\theta_l-\theta_m-\theta_i), \tag{1}$$

where $N$ is the number of oscillators, $\omega_i$ are natural frequencies that are drawn from a probability distribution $g(\omega)$, and $K_1$, $K_2$, and $K_3$ are the coupling strengths of the dyadic, triadic, and tetradic couplings, respectively. Later we will extend our results to random hypergraphs. The model (1) derives from the mean-field complex Ginzburg-Landau equation [22] or from weakly coupled Hopf bifurcations [23]. The model (1) has been studied in detail using the Ott-Antonsen approach in the limit $N \to \infty$ assuming Lorentzian-distributed natural frequencies [14]. It was shown that there is a bifurcation in the onset of synchronization from a gradual second-order transition to an explosive first-order transition. Here we use self-consistency to analyze these bifurcations for general symmetric natural frequency distributions $g(\omega)$. For instance, using a Gaussian distribution with mean zero and variance $\sigma^2 = 0.1$, Fig. 1 shows bifurcations from gradual (continuous) to explosive (discontinuous) synchronization, quantified by the order parameter $r_1$ defined below and shown as a color scale from dark blue for $r_1 = 0$ (incoherent) to light yellow for $r_1 = 1$ (highly synchronized), as the parameters $K_1$, $K_2$, and $K_3$ are varied. We derive analytic expressions for the locations of these bifurcations.

Self-consistency has been used for subcases of the dynamics (1), for instance, using $K_1 = K_3 = 0$ [24] (where the dynamics are fundamentally different, i.e., the unstable branch at onset of explosive synchronization never reconnects via a pitchfork bifurcation), using $K_2 = 0$ [25] (in which case drifters can be ignored), and using $K_3 = 0$ to study oscillators with inertia [26], but so far the full system (1) has not been

*lauren.smith@auckland.ac.nz

 

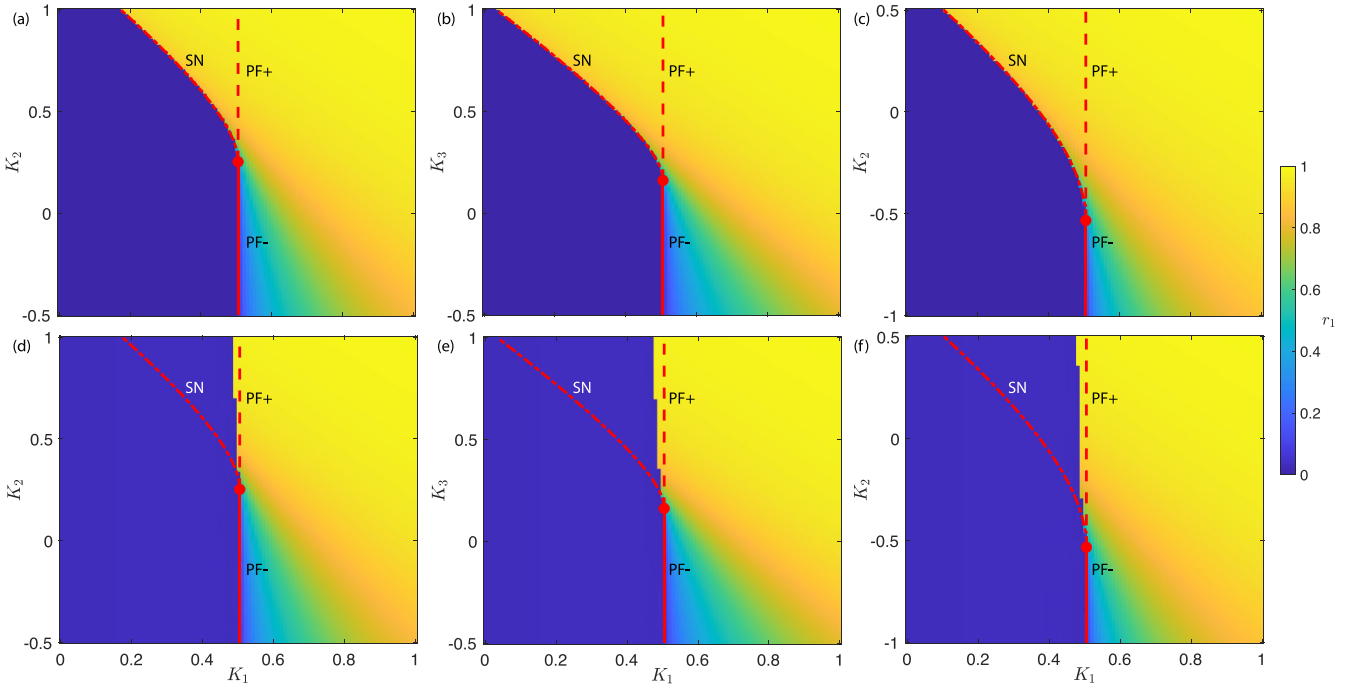


FIG. 1. Transitions between explosive and gradual synchronization, quantified by the order parameter $r_1$ (color scale from dark blue for $r_1 = 0$ to light yellow for $r_1 = 1$), for the higher-order system (1) with $N = 10^4$ and a Gaussian natural frequency distribution $g(\omega)$ with mean zero and variance $\sigma^2 = 0.1$. Theoretical bifurcation values, from (12) and (18), are shown as red curves, solid for supercritical pitchfork bifurcation (PF−), dashed for subcritical pitchfork bifurcation (PF+), and dot-dashed for saddle-node bifurcation (SN). The bifurcation curves meet at a codimension-2 bifurcation point given by (12) and (18) (red circle). (a)–(c) Highly synchronized initial condition. (d)–(f) Uniformly random initial condition. (a) and (d) $K_3 = 0$, with $K_1$ and $K_2$ varying. (b) and (e) $K_2 = 0$, with $K_1$ and $K_3$ varying. (c) and (f) $K_3 = 0.5$, with $K_1$ and $K_2$ varying.

studied via self-consistency and generic bifurcation sets have not been found.

We follow a similar self-consistency approach to that of Kuramoto [20], which has been generalized for several classes of higher-order interactions [24–29] [though not for (1)]. In the limit $N \to \infty$, the oscillator population is defined by a density $\rho(\theta, \omega, t)$, where $\rho(\theta, \omega, t)d\theta d\omega$ is the fraction of oscillators with phases in the range $(\theta, \theta + d\theta)$ and frequencies in the range $(\omega, \omega + d\omega)$ at time $t$. We will determine stationary distributions $\rho(\theta, \omega)$. To do so we write the dynamics (1) in mean-field form

$$\dot{\theta}_i = \omega_i + K_1 r_1 \sin(\Psi_1 - \theta_i) + K_2 r_1 r_2 \sin(\Psi_2 - \Psi_1 - \theta_i) + K_3 r_1^3 \sin(\Psi_1 - \theta_i), \tag{2}$$

where

$$r_1 e^{i\Psi_1} = \frac{1}{N}\sum_{j=1}^{N} e^{i\theta_j}, \quad r_2 e^{i\Psi_2} = \frac{1}{N}\sum_{j=1}^{N} e^{2i\theta_j} \tag{3}$$

denote the classical complex order parameter and a Daido order parameter [30], respectively. Assuming $g(\omega)$ is symmetric, in the limit $N \to \infty$ we find $\Psi_2 = \Psi_1$, and we can assume, without loss of generality, that $\Psi_1 = 0$. Thus the mean-field form (2) simplifies to

$$\dot{\theta}_i = \omega_i - \gamma \sin\theta_i, \tag{4}$$

where $\gamma = r_1(K_1 + K_2 r_2 + K_3 r_1^2)$. Equilibria of (4) satisfy

$$\omega_i = \gamma \sin\theta_i \tag{5}$$

for oscillators satisfying $|\omega_i| < \gamma$. Such oscillators form the synchronized cluster and are termed locked. Thus, the stationary density satisfies

$$\rho(\theta, \omega) = \delta(\omega - \gamma \sin\theta), \quad |\omega| < \gamma. \tag{6}$$

In partially synchronized states, there also exist "drifters" which do not synchronize and are those oscillators with frequencies $|\omega_i| > \gamma$. As in the Kuramoto model, stationarity of the drifter density requires that $\rho(\theta, \omega)$ is inversely proportional to the speed at $\theta$, i.e.,

$$\rho(\theta, \omega) = \frac{C(\omega, \gamma)}{|\omega - \gamma \sin\theta|}, \quad |\omega| > \gamma, \tag{7}$$

where $C(\omega, \gamma) = (2\pi)^{-1}\sqrt{\omega^2 - \gamma^2}$ is a normalization constant chosen such that $\int_{-\pi}^{\pi} \rho\, d\theta = 1$. The stationary density (6) and (7) shares a strong similarity to that of the original Kuramoto model [20,21], except with $Kr_1$ replaced by $\gamma$. The symmetries $\rho(-\theta, -\omega) = \rho(\theta, \omega)$ and $\rho(\theta + \pi, -\omega) = \rho(\theta, \omega)$ follow readily and are useful in our self-consistency analysis.

Self-consistency requires that the order parameters defined implicitly via (6) and (7) are consistent with the definitions in (3). Noting that $\Psi_1 = \Psi_2 = 0$, the equations are self-consistent provided

$$r_k = r_k^l + r_k^d, \quad k = 1, 2, \tag{8}$$

where $r_k^l$ and $r_k^d$ are the locked and drifter components of $r_k$, respectively. As in the case of the Kuramoto model, the

symmetries of $g(\omega)$ and $\rho(\theta,\omega)$ ensure that the imaginary parts of both the locked and drifter components are zero for all $k$. Focusing first on the locked component, using (6) we obtain

$$r_k^l = \int_{-\gamma}^{\gamma} \cos[k\theta(\omega)]g(\omega)d\omega = \gamma\int_{-\pi/2}^{\pi/2} \cos(k\theta)\cos(\theta)g(\gamma\sin\theta)d\theta, \tag{9}$$

where $\theta(\omega)$ is defined implicitly via (5). For the drifter component, using (7), we obtain

$$r_k^d = \int_{|\omega|>\gamma}\int_{-\pi}^{\pi} \cos(k\theta)g(\omega)\rho(\theta,\omega)d\theta\, d\omega. \tag{10}$$

Using the symmetries of $g$ and $\rho$, it is easily shown that $r_1^d = 0$ [31] and hence $r_1 = r_1^l$. However, $r_2^d \neq 0$, in fact, and after a change of variables $\eta = \omega/\gamma$, we obtain

$$r_2^d = 2\gamma\int_1^{\infty} I_\theta(\eta)g(\gamma\eta)d\eta, \tag{11}$$

where, assuming $\eta > 1$,

$$I_\theta(\eta) = \int_{-\pi}^{\pi}\cos(2\theta)\rho(\theta,\eta)d\theta = 1 + 2\eta(\sqrt{\eta^2-1}-\eta).$$

The combination of (8), (9), and (11) forms the self-consistency equations for the model (1). For given parameters $K_1$, $K_2$, and $K_3$, the solutions to the self-consistency equations give the order parameters $r_1$ and $r_2$ and hence the stationary density (6) and (7).

Having derived the self-consistency equations, we use them to determine bifurcations in the type of synchronization at onset. We use the general principle described in Ref. [32] to determine when the onset of synchronization bifurcates from gradual to explosive. Considering the values of $K_2$ and $K_3$ to be fixed, with $K_1$ varying, the incoherent state $r_1 = r_2 = 0$ is stable for small values of $K_1$, i.e., those less than some $K_c$, which may depend on $K_2$ and $K_3$. At the critical value $K_1 = K_c$, a branch of nonzero solutions for $r_1$ and $r_2$ emerges via a pitchfork bifurcation. If the pitchfork bifurcation is supercritical, i.e., the new solution branch exists for $K_1 > K_c$, then the new branch is stable, indicating the onset of stable synchronization via a (gradual) second-order phase transition. Conversely, if the pitchfork bifurcation is subcritical, i.e., the new solution branch exists for $K_1 < K_c$, then the new branch is unstable, which indicates an (explosive) first-order phase transition to synchronization must occur at $K_1 = K_c$, and the synchronized state will vanish via a saddle-node bifurcation at some value $K_1^{\mathrm{SN}}(K_2,K_3) < K_c$. In this case there is bistability in the parameter region $K_1^{\mathrm{SN}}(K_2,K_3) < K < K_c$, with both the incoherent and synchronized states being stable [cf. Figs. 1(a)–1(c) compared to Figs. 1(d)–1(f)]. Therefore, in order to determine when the onset of synchronization becomes explosive, it is sufficient to determine $K_c$ and whether the new nonzero branch of solutions for $r_1$ and $r_2$ exists for $K_1 > K_c$ or $K_1 < K_c$.

To determine $K_c$, we find the critical parameter at which the new nonzero branch emerges from the incoherent branch $r_1 = r_2 = 0$. Therefore, we consider the limit as $r_1, r_2 \to 0$ of solutions to (8). For $r_1 = r_1^l$ (9), assuming $r_1 \neq 0$, we can divide both sides of (9) by $r_1$ to obtain

$$1 = \left(K_1 + K_2 r_2 + K_3 r_1^2\right)\int_{-\pi/2}^{\pi/2}\cos^2(\theta)\, g(\gamma\sin\theta)d\theta.$$

In the limit $r_1, r_2 \to 0$ we obtain $1 = K_1\pi g(0)/2$ and hence the nonzero branch reaches zero at

$$K_1 = K_c = \frac{2}{\pi g(0)}, \tag{12}$$

which is identical to the critical coupling strength for the onset of synchronization in the classical Kuramoto model [20]. While we previously noted that $K_c$ may depend on $K_2$ and $K_3$, we find that it is independent of $K_2$ and $K_3$. Instead, we will show that $K_2$ and $K_3$ control whether the nonzero branching solution is stable or unstable and hence whether synchronization occurs gradually or abruptly.

We now determine the criticality of the pitchfork bifurcation at $K_1 = K_c$, with $K_1$ varying and $K_2$ and $K_3$ kept fixed. This will yield critical bifurcation parameters that separate explosive and gradual synchronization transitions. To do this, we expand the self-consistency equations (8), (9), and (11) in Taylor series about the critical point $(r_1, r_2, K_1) = (0, 0, K_c)$, with $K_2$ and $K_3$ treated as constants. The right-hand sides of the self-consistency equations (8) are functions of $\gamma$, and so we first expand about $\gamma = 0$ and then substitute $\gamma = K_c r_1 + r_1(K_1 - K_c) + K_2 r_1 r_2 + K_3 r_1^3$. For the locked components (9) we obtain

$$r_1 = r_1^l = \frac{1}{K_c}\gamma + \frac{\pi g''(0)}{16}\gamma^3 + O(\gamma^5), \tag{13}$$

$$r_2^l = \frac{2g(0)}{3}\gamma - \frac{g''(0)}{15}\gamma^3 + O(\gamma^5). \tag{14}$$

For the drifter component of $r_2$ (11) we obtain

$$r_2^d = -\frac{2g(0)}{3}\gamma + c_2\gamma^2 + O(\gamma^3), \tag{15}$$

where

$$c_2 = \frac{1}{2}\lim_{\gamma\to 0}\frac{d^2 r_2^d}{d\gamma^2} = 2\lim_{\gamma\to 0}\int_1^{\infty}\eta I_\theta(\eta)g'(\gamma\eta)d\eta. \tag{16}$$

Here we have used the fact that the integral $\int_1^{\infty} I_\theta(\eta)d\eta = -1/3$ converges, which allows us to apply the dominated convergence theorem to evaluate $\lim_{\gamma\to 0} r_2^d = 0$ and $\lim_{\gamma\to 0}\frac{dr_2^d}{d\gamma} = -\frac{2g(0)}{3}$. However, the integral $\int_1^{\infty}\eta I_\theta(\eta)d\eta$ diverges, meaning the limit and integral in (16) cannot be interchanged [31]. Physically, this reflects that the contribution of the drifters is not localized to $\omega = 0$ and the entirety of the natural frequency distribution $g(\omega)$ must be accounted for. We demonstrate this explicitly for two distributions with a common central region in Sec. SII of the Supplemental Material [31]. Combining (14) and (15), we obtain the expansion

$$r_2 = c_2\gamma^2 - \frac{g''(0)}{15}\gamma^3 + O(\gamma^5). \tag{17}$$

We now substitute $\gamma = K_c r_1 + r_1(K_1 - K_c) + K_2 r_1 r_2 + K_3 r_1^3$ into (13) and (17) and collect powers up to second order in $r_1$,

$r_2$, and $K_1 - K_c$, yielding

$$0 = \frac{1}{K_c}(K_1 - K_c) + \frac{K_2}{K_c}r_2 + \left(\frac{K_3}{K_c} + \frac{\pi K_c^3 g''(0)}{16}\right)r_1^2,$$
$$r_2 = c_2 K_c^2 r_1^2,$$

where we have first divided (13) through by $r_1$. Solving these equations simultaneously gives

$$r_1^2 = -\frac{16(K_1 - K_c)}{16\left(c_2 K_c^2 K_2 + K_3\right) + \pi K_c^4 g''(0)}.$$

From our previous discussion, the onset of synchronization will switch from gradual to explosive when this solution switches from existing to the right of $K_1 = K_c$ to existing to the left of $K_1 = K_c$, i.e., at the critical parameter values

$$c_2 K_c^2 K_2 + K_3 = K_{2,3}^* = -\frac{\pi K_c^4 g''(0)}{16}. \tag{18}$$

Assuming that $g''(0) < 0$, which is true for unimodal distributions, the onset of synchronization is gradual for $c_2 K_c^2 K_2 + K_3 < K_{2,3}^*$ and explosive for $c_2 K_c^2 K_2 + K_3 > K_{2,3}^*$.

From (18), if $K_2 = 0$, then the bifurcation is at $K_3 = K_{2,3}^*$, which does not depend on $c_2$ and only depends on $g(0)$ and $g''(0)$. This is similar to Kuramoto's result [20], in which bifurcation only depends on the shape of $g$ at 0. The cause of this is that the drifters can be neglected if $K_2 = 0$ [25], whereas the drifters have a non-negligible effect, quantified by $c_2$, if $K_2 \neq 0$.

We now demonstrate our results explicitly, first for Lorentzian-distributed natural frequencies and then for Gaussian-distributed natural frequencies. For a Lorentzian distribution centered at zero and with spread $\Delta = 1$ we have $g(\omega) = [\pi(1 + \omega^2)]^{-1}$. Evaluating the self-consistency integrals (9) and (11) directly yields

$$r_1 = \frac{\sqrt{1+\gamma^2} - 1}{\gamma}, \quad r_2 = \frac{2 + \gamma^2 - 2\sqrt{1+\gamma^2}}{\gamma^2} = r_1^2.$$

The first equation can be solved for $\gamma$, which yields $\gamma = 2r_1/(1 - r_1^2)$. We also have our definition $\gamma = r_1(K_1 + K_2 r_2 + K_3 r_1^2)$. Solving this system of equations for $r_1$ yields

$$0 = r_1\left[-2 + K_1\left(1 - r_1^2\right) + K_{2+3}r_1^2\left(1 - r_1^2\right)\right], \tag{19}$$

where $K_{2+3} = K_2 + K_3$, as defined in Ref. [14]. Equation (19) is identical to the equivalent equation obtained via the Ott-Antonsen approach [14], which has been shown to agree with the full dynamics (1) for large $N$. For the Lorentzian distribution we obtain $K_c = 2$, meaning that the new branch of nonzero solutions $r_1$ and $r_2$ emanates from $K_1 = K_c = 2$. We also directly compute $c_2 = 1/4$ and $K_{2,3}^* = 2$ and hence our criticality condition (18) becomes $K_{2+3} = K_{2,3}^* = 2$. Our results agree with the analysis using the Ott-Antonsen approach [14], which finds a codimension-2 bifurcation at $(K_1, K_{2+3}) = (2, 2)$ such that at bifurcation the pitchfork bifurcation changes criticality and a saddle-node bifurcation emerges.

We now consider Gaussian-distributed natural frequencies, with mean zero and variance $\sigma^2$ (in our numerical examples we use $\sigma^2 = 0.1$). We can again directly integrate the self-consistency integrals (9) and (11) to obtain

$$r_1 = \frac{\sqrt{\pi}}{2}Ae^{-A^2/2}[I_0(A^2/2) + I_1(A^2/2)], \tag{20}$$

$$r_2 = 1 + \frac{e^{-A^2} - 1}{A^2}, \tag{21}$$

where $A = \gamma/\sqrt{2}\sigma$ and $I_n$ denotes the $n$th modified Bessel function of the first kind. In principle, Eq. (21) can be solved for $A$ and then the result is substituted into (20), which can then be solved for $r_1$; however, that is not possible in practice, except numerically. We note that the relation $r_2 = r_1^2$ that was true for the Lorentzian distribution, which allowed the simplification of $K_2$ and $K_3$ to the combined variable $K_{2+3}$, is not true for Gaussian distributions. This is reflected in Fig. 1 by the differences between Figs. 1(a) and 1(d) and Figs. 1(b) and 1(e). For our criticality results, we find $K_c = 2\sigma\sqrt{2/\pi}$, $c_2 = 1/4\sigma^2$, and $K_{2,3}^* = 2\sigma\sqrt{2/\pi^3}$. The red curves in Fig. 1 show that these theoretical values agree well with numerical simulations of the full model (1). Our numerical results show that the onset of synchronization from a random initial condition [Figs. 1(d)–1(f)] occurs at $K_1 = K_c = 0.5046$ via a pitchfork bifurcation, with a switch from gradual to explosive synchronization as $K_2$ or $K_3$ is increased, corresponding to the change in criticality of the pitchfork bifurcation [shown as solid for supercritical (PF−) and dashed for subcritical (PF+)]. From (12) and (18), for $K_3 = 0$ [Figs. 1(a) and 1(d)] this codimension-2 bifurcation occurs at $(K_1, K_2) = (K_c, K_{2,3}^*/c_2K_c^2) = (0.5046, 0.2523)$. For $K_2 = 0$ [Figs. 1(b) and 1(e)] the codimension-2 bifurcation occurs at $(K_1, K_3) = (K_c, K_{2,3}^*) = (0.5046, 0.1606)$ and for $K_3 = 0.5$ [Figs. 1(c) and 1(f)] the codimension-2 bifurcation occurs at $(K_1, K_2) = (K_c, (K_{2,3}^* - 0.5)/c_2K_c^2) = (0.5046, -0.5331)$

When the onset to synchronization is explosive, i.e., when $c_2 K_c^2 K_2 + K_3 > K_{2,3}^*$, the branch of nonzero solutions for $r_1$ and $r_2$ that emanate from $K_1 = K_c$ are unstable, and there is a saddle-node bifurcation that occurs at some $K_1^{\mathrm{SN}}(K_2, K_3)$ such that the unstable branch meets a stable branch of synchronized solutions. For Lorentzian-distributed natural frequencies the saddle-node bifurcation can be found easily by directly solving (19) [14]. However, for Gaussian-distributed natural frequencies the same approach would require analytically solving (20) and (21), which is not possible. As a method to (numerically) find the saddle-node bifurcation for general frequency distributions, we recognize that our self-consistency equations (8)–(11) are of the form $r_1 = r_1(\gamma) = \gamma F_1(\gamma)$ and $r_2 = r_2(\gamma)$. From the definition of $\gamma$, this sets up a single self-consistency equation for $\gamma$,

$$\gamma = r_1(\gamma)[K_1 + K_2 r_2(\gamma) + K_3 r_1(\gamma)^2],$$

which has solutions $\gamma = 0$ and $\gamma$ satisfying

$$0 = F_1(\gamma)[K_1 + K_2 r_2(\gamma) + K_3 \gamma^2 F_1(\gamma)^2] - 1 = H(\gamma). \tag{22}$$

Each positive root of $H(\gamma)$ corresponds to a solution branch of the self-consistency equations (8)–(11). Thus, finding the saddle-node bifurcation is equivalent to finding double roots of $H$, i.e., solutions to $H(\gamma) = 0$ and $H'(\gamma) = 0$. For Gaussian natural frequencies $H(\gamma)$ is obtained from (20) and (21) and

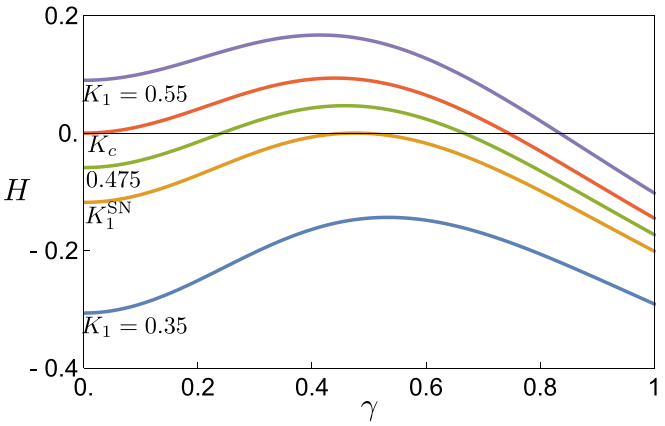


FIG. 2. Plot of $H(\gamma)$ given by (22) for Gaussian-distributed natural frequencies with mean zero and variance $\sigma^2 = 0.1$ using $K_2 = 0.5$, $K_3 = 0$, and a range of $K_1$ values (labeled in the figure near the vertical axis).

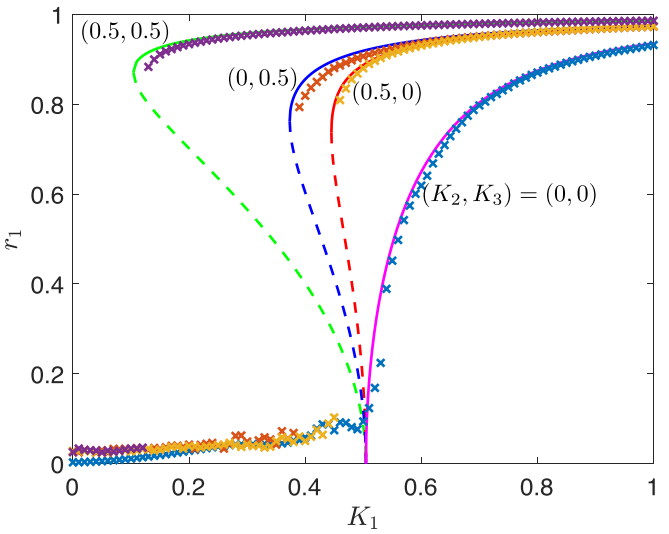


FIG. 3. Order parameter $r_1$ as $K_1$ is varied for Gaussian-distributed natural frequencies with variance $\sigma^2 = 0.1$, for $K_2 \in \{0, 0.5\}$ and $K_3 \in \{0, 0.5\}$ [labeled in the figure as pairs $(K_2, K_3)$]. Results are shown for the thermodynamic limit with all-to-all coupling (solid curves for stable and dashed curves for unstable solutions), solving (20) and (21), as well as simulations of (23) for a random hypergraph (crosses) with $N = 10^3$, $p_k = 0.1/N^{k-1}$, and renormalized coupling strengths $K'_k = K_k/p_k$.

shown in Fig. 2 for a range of $K_1$ values with $K_2 = 0.5$ and $K_3 = 0$ kept fixed. At $K_1 = 0.35$ (bottom curve) there are no roots and hence no synchronized solution. Increasing $K_1$, at $K_1^{SN} = 0.445$, $H(\gamma)$ has a double root, indicating a saddle-node bifurcation and birth of a synchronized state via an explosive transition. For $K_1^{SN} < K_1 < K_c = 0.505$, $H(\gamma)$ has two roots: one stable and one unstable synchronized solution. For $K_1 > K_c$, there is a single root of $H(\gamma)$; the unstable solution has been destroyed in the pitchfork bifurcation at $K_1 = K_c$. We have numerically found the saddle-node bifurcation $K_1^{SN}(K_2, K_3)$ for Gaussian natural frequencies for a range of $K_1$, $K_2$, and $K_3$ values, as shown in Fig. 1 by the dot-dashed curves. Our results show excellent agreement with the explosive transitions from synchronized to incoherent states.

We now extend our results to random hypergraphs. Consider the dynamics

$$\dot{\theta}_i = \omega_i + \frac{K_1}{N}\sum_{j=1}^{N} A_{ij}\sin(\theta_j - \theta_i) + \frac{K_2}{N^2}\sum_{j,l=1}^{N} B_{ijl}\sin(2\theta_j - \theta_l - \theta_i) + \frac{K_3}{N^3}\sum_{j,l,m=1}^{N} C_{ijlm}\sin(\theta_j + \theta_l - \theta_m - \theta_i), \tag{23}$$

where $A$, $B$, and $C$ are the adjacency matrices or tensors encoding dyadic, triadic, and tetradic couplings, respectively. As a higher-order extension to Erdős-Rényi graphs, we consider the case such that each $A_{ij}$, $B_{ijl}$, and $C_{ijlm}$ is independently random with probabilities $p_1$, $p_2$, and $p_3$ of being equal to 1, respectively; otherwise they are zero. In the thermodynamic limit, the dynamics of (23) with a random hypergraph is identical to that of an all-to-all coupled network, with weighted adjacency matrices or tensors $A_{ij} = p_1$, $B_{ijl} = p_2$, and $C_{ijlm} = p_3$ for all $i, j, l, m$. As such, upon renormalizing the coupling strengths $K'_k = K_k/p_k$, the dynamics of (1) and (23) are identical in the thermodynamic limit. This is demonstrated in Fig. 3, which shows that the order parameter $r_1$ obtained by simulating (23) with $N = 10^3$ and $p_k = 0.1/N^{k-1}$, such that the mean degrees are $\langle d^k \rangle = 100$, closely agrees with $r_1$ obtained by solving the self-consistency equations (20) and (21) for a range of coupling strengths. In particular, the (saddle-node and pitchfork) bifurcations and their criticalities given by (12), (18), and (22) apply also to random hypergraphs, provided the coupling strengths $K_k$ are renormalized by the probabilities $p_k$. This has been shown previously for Lorentzian-distributed natural frequencies using the Ott-Antonsen ansatz [14] and is extended here to general symmetric natural frequency distributions.

In summary, we have found critical synchronization transitions for networks of coupled oscillators with generic symmetric natural frequency distributions via a self-consistency approach. Our analysis shows that drifters play a crucial role in controlling synchronization bifurcations, and so the whole natural frequency distribution must be accounted for. This is unlike most other self-consistency analyses, in which the drifters can be neglected and hence bifurcations are determined exclusively by the shape of the distribution at its center. We have shown the efficacy of our methodology for both Lorentzian and Gaussian natural frequency distributions and both all-to-all and random hypergraphs.

Our methodology can be readily extended to a broad class of possible higher-order interactions, with the only requirement being that the mean-field dynamics can be written in the form (4) for some $\gamma$ that encodes the relevant Daido order parameters and their weightings, in particular, for coupling functions of the form $\sin(-\theta_i + \sum_{p=1}^{P}\sum_{q=1}^{Q_p} a_p s_{p,q}\theta_{j_{p,q}})$, where the $a_p$ are positive integers, $s_{p,q} = \pm 1$, and $j_{p,q}$ are indices that are summed over. To ensure diffusive-type

dynamics, we require $-1 + \sum_p \sum_q a_p s_{p,q} = 0$. The contribution to $\gamma$ from such a coupling function is $\prod_{p=1}^{P} r_{a_p}^{b_p}$, where $b_p = \sum_q |s_{p,q}|$. For example, the coupling function $\sin(2\theta_j - \theta_l - \theta_i)$ has $M = 2$, $a_1 = 2$, $s_{1,1} = 1$, $a_2 = 1$, and $s_{2,1} = -1$. The contribution to $\gamma$ from this term is $r_2 r_1$. The self-consistency analysis proceeds by applying our methodology discussed herein to solve for the relevant Daido order parameters.


[1] D. Bhowmik and M. Shanahan, in *Proceedings of the International Joint Conference on Neural Networks (IJCNN), Brisbane, 2012* (IEEE, Piscataway, 2012).

[2] C. Bick, M. Goodfellow, C. R. Laing, and E. A. Martens, Understanding the dynamics of biological and neural oscillator networks through exact mean-field reductions: A review, J. Math. Neurosc. **10**, 9 (2020).

[3] J. Machowski, J. W. Bialek, and J. Bumby, *Power System Dynamics: Stability and Control* (Wiley, New York, 2011).

[4] T. Nishikawa and A. E. Motter, Comparative analysis of existing models for power-grid synchronization, New J. Phys. **17**, 015012 (2015).

[5] G. Filatrella, A. H. Nielsen, and N. F. Pedersen, Analysis of a power grid using a Kuramoto-like model, Eur. Phys. J. B **61**, 485 (2008).

[6] B. Schäfer and G. C. Yalcin, Dynamical modeling of cascading failures in the Turkish power grid, Chaos **29**, 093134 (2019).

[7] G. Petri, P. Expert, F. Turkheimer, R. Carhart-Harris, D. Nutt, P. J. Hellyer, and F. Vaccarino, Homological scaffolds of brain functional networks, J. R. Soc. Interface **11**, 20140873 (2014).

[8] L.-D. Lord, P. Expert, H. M. Fernandes, G. Petri, T. J. Van Hartevelt, F. Vaccarino, G. Deco, F. Turkheimer, and M. L. Kringelbach, Insights into brain architectures from the homological scaffolds of functional connectivity networks, Front. Syst. Neurosci. **10**, 85 (2016).

[9] F. Battiston, E. Amico, A. Barrat, G. Bianconi, G. Ferraz de Arruda, B. Franceschiello, I. Iacopini, S. Kéfi, V. Latora, Y. Moreno, M. M. Murray, T. P. Peixoto, F. Vaccarino, and G. Petri, The physics of higher-order interactions in complex systems, Nat. Phys. **17**, 1093 (2021).

[10] S. Majhi, M. Perc, and D. Ghosh, Dynamics on higher-order networks: A review, J. R. Soc. Interface **19**, 20220043 (2022).

[11] F. Battiston, G. Cencetti, I. Iacopini, V. Latora, M. Lucas, A. Patania, J.-G. Young, and G. Petri, Networks beyond pairwise interactions: Structure and dynamics, Phys. Rep. **874**, 1 (2020).

[12] P. S. Skardal and A. Arenas, Abrupt desynchronization and extensive multistability in globally coupled oscillator simplexes, Phys. Rev. Lett. **122**, 248301 (2019).

[13] A. P. Millán, J. J. Torres, and G. Bianconi, Explosive higher-order Kuramoto dynamics on simplicial complexes, Phys. Rev. Lett. **124**, 218301 (2020).

[14] P. S. Skardal and A. Arenas, Higher order interactions in complex networks of phase oscillators promote abrupt synchronization switching, Commun. Phys. **3**, 218 (2020).

[15] S. Adhikari, J. G. Restrepo, and P. S. Skardal, Synchronization of phase oscillators on complex hypergraphs, Chaos **33**, 033116 (2023).

[16] Y. Zhang, M. Lucas, and F. Battiston, Higher-order interactions shape collective dynamics differently in hypergraphs and simplicial complexes, Nat. Commun. **14**, 1605 (2023).

[17] Z. Gao, D. Ghosh, H. A. Harrington, J. G. Restrepo, and D. Taylor, Dynamics on networks with higher-order interactions, Chaos **33**, 040401 (2023).

[18] E. Ott and T. M. Antonsen, Low dimensional behavior of large systems of globally coupled oscillators, Chaos **18**, 037113 (2008).

[19] E. Ott and T. M. Antonsen, Long time evolution of phase oscillator systems, Chaos **19**, 023117 (2009).

[20] Y. Kuramoto, *Chemical Oscillations, Waves, and Turbulence* (Springer, Berlin, 1984).

[21] S. H. Strogatz, From Kuramoto to Crawford: Exploring the onset of synchronization in populations of coupled oscillators, Physica D **143**, 1 (2000).

[22] I. León and D. Pazó, Phase reduction beyond the first order: The case of the mean-field complex Ginzburg-Landau equation, Phys. Rev. E **100**, 012211 (2019).

[23] P. Ashwin and A. Rodrigues, Hopf normal form with $S_N$ symmetry and reduction to systems of nonlinearly coupled phase oscillators, Physica D **325**, 14 (2016).

[24] X. Wang, Z. Zheng, and C. Xu, Collective dynamics of phase oscillator populations with three-body interactions, Phys. Rev. E **104**, 054208 (2021).

[25] C. Xu, Y. Zhai, Y. Wu, Z. Zheng, and S. Guan, Enhanced explosive synchronization in heterogeneous oscillator populations with higher-order interactions, Chaos Soliton. Fract. **170**, 113343 (2023).

[26] N. G. Sabhahit, A. S. Khurd, and S. Jalan, Prolonged hysteresis in the Kuramoto model with inertia and higher-order interactions, Phys. Rev. E **109**, 024212 (2024).

[27] X. Wang, C. Xu, and Z. Zheng, Phase transition and scaling in Kuramoto model with high-order coupling, Nonlinear Dyn. **103**, 2721 (2021).

[28] C. Xu, X. Wang, and P. S. Skardal, Bifurcation analysis and structural stability of simplicial oscillator populations, Phys. Rev. Res. **2**, 023281 (2020).

[29] C. Xu and P. S. Skardal, Spectrum of extensive multiclusters in the Kuramoto model with higher-order interactions, Phys. Rev. Res. **3**, 013013 (2021).

[30] H. Daido, Multibranch entrainment and scaling in large populations of coupled oscillators, Phys. Rev. Lett. **77**, 1406 (1996).

[31] See Supplemental Material at http://link.aps.org/supplemental/10.1103/PhysRevE.109.L022202 for full details of the effects of drifters on the order parameters, including an explicit example showing that they cannot be neglected.

[32] C. Kuehn and C. Bick, A universal route to explosive phenomena, Sci. Adv. **7**, eabe3824 (2021).